

Article

The Effect of NNK, A Tobacco Smoke Carcinogen, on the miRNA and Mismatch DNA Repair Expression Profiles in Lung and Head and Neck Squamous Cancer Cells

Sotirios G. Doukas ^{1,2}, Dimitra P. Vageli ^{2,*} , George Lazopoulos ³, Demetrios A. Spandidos ⁴, Clarence T. Sasaki ² and Aristidis Tsatsakis ¹ 

¹ Department of Forensic Sciences and Laboratory of Toxicology, Medical School, University of Crete, 71003 Heraklion, Greece; sotirios.doukas.mail@gmail.com (S.G.D.); tsatsaka@uoc.gr (A.T.)

² Department of Surgery, The Yale Larynx Laboratory, New Haven, CT 06510, USA; clarence.sasaki@yale.edu

³ Department of Cardiothoracic Surgery, Medical School, University of Crete, 71110 Heraklion, Greece; g.lazopoulos@med.uoc.gr

⁴ Laboratory of Clinical Virology, Medical School, University of Crete, 71110 Heraklion, Greece; spandidos@spandidos.gr

* Correspondence: dimitra.vangeli@yale.edu; Tel.: +(203)-737-1447

Received: 8 February 2020; Accepted: 19 April 2020; Published: 21 April 2020



Abstract: Tobacco smoking is a common risk factor for lung cancer and head and neck cancer. Molecular changes such as deregulation of miRNA expression have been linked to tobacco smoking in both types of cancer. Dysfunction of the Mismatch DNA repair (MMR) mechanism has also been associated with a poor prognosis of these cancers, while a cross-talk between specific miRNAs and MMR genes has been previously proposed. We hypothesized that exposure of lung and head and neck squamous cancer cells (NCI and FaDu, respectively) to tobacco-specific nitrosamine 4-(methylnitrosamino)-1-(3-pyridyl)-1-butanone (NNK) is capable of altering the expression of MSH2 and MLH1, key MMR components, by promoting specific miRNA deregulation. We found that either a low (1 μ M) or high (2 μ M) dose of NNK induced significant upregulation of “oncomirs” miR-21 and miR-155 and downregulation of “tumor suppressor” miR-422a, as well as the reduction of MMR protein and mRNA expression, in NCI and FaDu, compared to controls. Inhibition of miR-21 restored the NNK-induced reduced MSH2 phenotype in both NCI and FaDu, indicating that miR-21 might contribute to MSH2 regulation. Finally, NNK exposure increased NCI and FaDu survival, promoting cancer cell progression. We provide novel findings that deregulated miR-21, miR-155, and miR-422a and MMR gene expression patterns may be valuable biomarkers for lung and head and neck squamous cell cancer progression in smokers.

Keywords: tobacco smoke; NNK; head and neck cancer; lung cancer; Mismatch DNA repair; MSH2; MLH1; miR-21; miR-155; miR-422a

1. Introduction

Plenty of epidemiologic data have shown the association of tobacco smoking with the development of human malignancies [1,2]. Although the antismoking campaign in multiple countries has shown positive results, the rate of smokers in both the United States and Europe remains significant [3–5]. It is estimated that nearly 40 percent of diagnosed cancers are directly or indirectly related to tobacco smoking [6].

Lung cancer has the highest mortality rates in the world for both men and women, and is the most common type of malignancy in men [7]. In addition, head and neck cancer, and especially head

and neck squamous cell carcinoma (HNSCC), represents one of the most aggressive malignancies with a high rate of mortality. [8,9]. Tobacco smoking has been one of the most well-established risk factors for both lung and head and neck cancers [1–8]. It is known that tobacco smoke contains a mixture of thousands of compounds, including a large number of known carcinogens [2]. It is believed that exposure of cells to tobacco smoke carcinogens can lead to DNA damage, which may cause chromosomal instability and increased cell proliferation [10–13]. In particular, tobacco-specific nitrosamine 4-(methylnitrosamino)-1-(3-pyridyl)-1-butanone (NNK), which is one of the chemicals in tobacco smoke, has been linked to lung and head and neck cancer [14], and has also been shown to upregulate oncogenic pathways [15–17].

The development and progression of lung and head and neck malignancies appear to be a complex process. Although multiple diagnostic and prognostic markers have been identified for both lung and head and neck cancers [18,19], the precise molecular mechanisms involved in the development and progression of these malignancies remain unclear.

We understand that a functional DNA repair mechanism that includes the recognition and repair of mismatch DNA errors during DNA replication is essential in eliminating the harmful effect of several environmental risk factors, such as NNK, on the exposed cells [20–23]. A number of studies have shown that reduced expression of mismatch DNA repair (MMR) genes increases the incidence of microsatellite instability [24–27], which is often found in head and neck cancer [28–31]. Other studies have also shown that reduced expression of *MSH2* or *MLH1* genes at the protein or mRNA levels is associated with poor survival and MSI in lung cancer [32–34].

In addition, MMR deficiency appears to affect the effectiveness of chemotherapy in these cancers [34,35]. Also, MMR status has been shown to influence the effectiveness of target immunotherapy, including PD-1 and PD-L1 inhibitors, for lung and head and neck cancers [36]. Therefore, several studies have focused on the assessment of the MMR status, as this may have a significant predictive value for these patients. [23,24,34,36,37].

A number of regulatory molecules such as miRNAs have been suggested to be implicated in the regulation of MMR genes [38–46]. In particular, recent studies support a cross-talk between specific miRNAs and MMR genes [41–43]. It has been suggested that tumor suppressor miRNA-422a plays an important regulatory role in *MLH1* expression, which is responsible for repairing DNA damage [44]. Some reports have also shown that oncomir miR-21 downregulates *hMSH2* gene expression by targeting the 3' untranslated region of its mRNA [45], and that miR-155 can significantly downregulate *hMSH2*, *hMSH6*, and *hMLH1* [46], while others have suggested that miRNAs play an important role in modulating cell cycle progression by targeting *hMSH2* in lung cancer [42]. Although there are reports suggesting a relationship between the MMR mechanism and miRNA profiles [41,43,44,46], the underlying molecular mechanism by which tobacco smoke carcinogens induce miRNA deregulation and affect the expression profiles of mismatch repair genes, particularly in lung and head and neck cancer, is not yet known.

Here, we attempt to explore whether NNK affects the expression of small regulatory molecules, such as known miRNA markers, previously associated with upper aerodigestive tract malignancies [47–54] that may directly or indirectly be involved in the regulation for MMR expression phenotypes. Understanding the molecular changes induced by various risk factors, such as tobacco smoke, which promote the development and progression of cancer, will help to develop new diagnostic and therapeutic approaches [55,56], leading to optimization of their management.

2. Materials and Methods

2.1. Cell Culture and Treatment Conditions

2.1.1. Human Hypopharyngeal and Lung Squamous Cancer Cell Culture

Human hypopharyngeal squamous cancer cells (HSCC), FaDu (HTB-43), were provided by ATCC, Manassas, VA, USA, and cultured in Eagle's Minimum Essential Medium (EMEM, ATCC, Manassas,

VA, USA), 10% FBS, 1% pen/strep, at 37 °C in humidified air and 5% CO₂. Human lung squamous cancer cells (LSCC), NCI (NCI-H1703), were provided by ATCC, Manassas, VA, USA, and cultured in RPMI-1640 medium (ATCC, Manassas, VA, USA) 10% FBS, 1% pen/strep, at 37 °C in humidified air and 5% CO₂.

2.1.2. Treatment Conditions

Cancer cells reached 70–80% confluency and were then exposed to experimental media for 24 h. Experimental groups included exposure to (i) 1 µM and (ii) 2 µM of 4-(*N*-Methyl-*N*-Nitrosamino)-1-(3-pyridyl)-1-butanone (CAS 64091-91-4) or NNK (sc-209854 Santa-Cruz®, Dallas, TX, USA) [17] (NNK dissolved in DMSO-vehicle as 1 M stock solution). Cells were incubated in serum-free medium (EMEM for FaDu and RPMI-1640 for NCI, with 1% pen/strep) with NNK, at 37 °C in humidified air and 5% CO₂. The untreated control groups for each cancer cell line, NCI and FaDu, consisted of cells incubated in serum-free media (EMEM or RPMI-1640, 1% pen/strep, with the vehicle but without NNK). Experimental and control groups were cultured in parallel for each cancer cell line. All the experiments were independently repeated three times. Cells were harvested at the end of the treatment cycle.

2.2. Immunoperoxidase Cell Staining for MSH2

We performed an immunocytochemical analysis to detect nuclear and cytoplasmic MSH2 levels in NCI and FaDu cells exposed to NNK relative to untreated controls. Specifically, NCI and FaDu were grown on slides (multiwall chamber slides; Nunc™ Lab-Tek™, Thermo Scientific, Waltham, MA, USA) and treated with experimental media of 1 µM or 2 µM NNK. Untreated controls were also used for each cancer cell line.

Cells were fixed immediately after the final exposure to experimental or control media in 4% paraformaldehyde for 10 min, followed by 3 washes with PBS and permeabilization of the cell membranes using 0.02% Triton X100-PBS (AmericanBio, Natick, MA, USA) for 3 min. Cells were incubated with 0.5% H₂O₂ in PBS for 10 min, followed by 2 washes with PBS and blocking with 5% bovine serum albumin (BSA)-PBS (Sigma-Aldrich, St. Louis, MO, USA) for 1 h, and incubation with 1:100 primary mouse-monoclonal antibody HRP for DNA mismatch repair protein MSH2 (MutS protein homolog 2, MSH2_HUMAN, Clone D-6, Santa Cruz Biotechnology, Inc., Dallas, TX, USA), for 1 h at 37 °C. Cells were washed in 1% Tween-PBS and incubated to 1:100 dilutions of secondary mouse-IgGκ BP-HRP (Santa Cruz Biotechnology Inc., Dallas, TX, USA), for 30 min at 37 °C. Subsequently, cells were incubated for 1 min with freshly mixed DAB (3,3' Diaminobenzidine Tetrahydrochloride in 0.1 M Tris-HCl pH 7.6) with 0.5% hydrogen peroxide, washed in distilled H₂O and counterstained with Gill's Hematoxylin Solution, No. 2 (Santa Cruz Biotechnology Inc., Dallas, TX, USA) for 5 s. Finally, cells were washed with several changes of distilled H₂O and dehydrated in graded alcohols, cleared with xylene and mounted with permanent mounting medium and coverslip.

Slides were examined using a Leica light microscope and images were captured by Aperio CS2 and analyzed by Image Scope software [57]. Expression levels of nuclear MSH2, in experimental and control NCI and FaDu groups, were assigned as positivity [Np/Nt = Number of nuclear positive/total number of nuclei, means (SD)] from at least two independent images (≥10 cells).

2.3. Immunofluorescence Cell Staining for MLH1

We performed an immunofluorescence assay to detect nuclear and cytoplasmic MLH1 levels in NCI and FaDu cells exposed to NNK relative to untreated controls. Specifically, NCI and FaDu were grown on slides (multiwall chamber slides; Lab-Tek®) and treated with experimental media of 1 µM and 2 µM NNK. Untreated controls were also used for each cancer cell line.

Cells were fixed immediately after the final exposure to experimental or control media in 4% paraformaldehyde for 10 min, followed by 3 washes with PBS and permeabilization of cell membranes using 0.02% Triton X100-PBS (AmericanBio, Natick, MA, USA) for 3 min, blocking with 2% bovine serum albumin (BSA)-PBS (Sigma-Aldrich) for 1 h, and incubation with 1:50 of primary mouse-monoclonal

antibody for DNA mismatch repair protein MLH1 (MutL protein homolog 1, MLH1 HUMAN, Clone A-8, Santa Cruz Biotechnology Inc., Dallas, TX, USA), overnight at 4 °C. Cells were washed in 1% Tween-PBS and incubated with 1:500 dilutions of secondary antimouse DyLight[®]488 (green; Vector Labs, Burlingame, CA, USA), for 1 h, at room temperature. Finally, cells were mounted using Prolong Gold Mountant with diamidino-phenylindole (ProLong[®] Diamond Antifade Mountant with DAPI; Life Technologies, Thermo Scientific, Franklin, MA, USA) for nuclear staining of cells (blue).

Slides were examined using a Zeiss Confocal microscope and images were captured and analyzed using the Zen imaging software from Carl Zeiss, microscopy, Germany, as previously described [58,59]. Expression levels of nuclear MLH1, in experimental and control NCI and FaDu groups, were identified by fluorescence intensity [MLH1/DAPI means(SD) bin count] from four independent images (≥ 10 cells) (Zen imaging software, Carl Zeiss, microscopy GmbH, Jena, Germany).

2.4. Western Blotting for MMR Proteins

We performed a Western blot analysis to determine the expression levels of MSH2 and MLH1 nuclear and cytoplasmic proteins in experimental and control NCI and FaDu groups. We used β -actin and Histone 1 to normalize cytoplasmic and nuclear extracts, respectively, and expression levels were estimated using the Image Lab 5.2 analysis software (Bio-Rad, Hercules, CA, USA), as previously described [59,60]. Specifically, 20 to 30 μ g of nuclear and cytoplasmic NCI and FaDu protein extracts were heated at 70 °C for 10 min in sodium dodecyl sulfate-polyacrylamide gel electrophoresis Laemmli sample buffer (Bio-Rad, Hercules, CA, USA), and separated using 420–% Mini-PROTEAN TGX Tris/Glycine precast gels, at 150V for 1 h. We used precision plus prestained protein standards (Dual Color or Kaleidoscope, BIO-RAD) as molecular-weight size markers. Proteins were transferred onto a 0.45 mm nitrocellulose membrane, using a Trans-Blot Turbo transfer system (Bio-Rad). After blocking in 5% BSA, for 1 h, membranes were incubated with 1:300 primary antibodies, MSH2 (Clone D-6) and MLH1 (Clone A-8) (Santa Cruz Biotechnology Inc., Dallas, TX, USA), which were diluted in 5% BSA, overnight at 4 °C. Membranes were incubated for 1:30 h with goat antimouse horseradish peroxidase-conjugated secondary antibodies (EMD Millipore, Burlington, MA, USA) at 1:2000, and chemiluminescence was determined using an enhanced chemiluminescence detection system (Clarity Western ECL Substrate, Bio-Rad). Membranes were also stripped using RestoreTM Western Blot Stripping buffer (Pierce Biotechnology, Rockford, IL, USA) and reported with β -actin (C4; Santa Cruz Biotechnology Inc., Dallas, TX, USA) for cytoplasmic extracts and Histone 1 (AE-4; Santa Cruz Biotechnology Inc., Dallas, TX, USA) for nuclear extracts normalization. Protein levels were quantified by the Gel imaging system (Bio-Rad, Hercules, CA, USA) in each nuclear or cytoplasmic cellular compartment (Image Lab 5.2 analysis software, Bio-Rad, Hercules, CA, USA).

2.5. Quantitative Real-Time PCR for hMSH2 and hMLH1

We used a real-time quantitative polymerase chain reaction (qPCR) analysis to evaluate the transcriptional levels of *hMSH2* and *hMLH1*. Total RNA (RNeasy mini kit; Qiagen Inc., Valencia, CA, USA) was isolated from NCI and FaDu exposed to 1 μ M or 2 μ M of NNK and their corresponding untreated controls. Briefly, we determined RNA quality and concentration by absorption ratios at 260/280 nm (>2.0) and 260 nm, respectively (NanoDropTM 1000 spectrophotometer; Thermo Fisher Scientific, Waltham, MA, USA). We performed reverse transcription (iScript cDNA synthesis kit; Bio-Rad) from total RNA and real-time qPCR analysis (Bio-Rad real-time thermal cycler CFX96TM; Bio-Rad) using specific primers for target genes and reference housekeeping gene, human glyceraldehyde 3-phosphate dehydrogenase (*hGAPDH*) (QuantiTect Primers Assays; Qiagen) (Supplementary Table S1), and iQTM SYBR Green Supermix (Bio-Rad). We performed assays on 96-well plates, in triplicate for each sample, and data were analyzed using the CFX96TM software [59,60]. Relative mRNA expression levels were estimated for each target gene compared to the reference control gene ($\Delta\Delta C_t$).

2.6. miRNA Analysis for miR-21, miR-155 and miR-422a

We performed a miRNA analysis by qPCR to show the expression of “oncomirs” miR-21 and miR-155, and “tumor suppressor” miR-422a, and to monitor the effect of 1 μ M and 2 μ M of NNK on NCI and FaDu treated cells, compared to their corresponding untreated controls. We used miScript II RT kit (Qiagen) to perform reverse transcription synthesis of miRNAs from total RNA (isolated for miRNA analysis as described above) according to the manufacturer’s instructions, using specific primers for target miRNAs of the human genome and normalization control small RNA RNU6B (snRNA RNU62–) (miScript Primer Assay; miScript SYBR Green PCR Kit; Qiagen, Louisville, KY, USA) (Supplementary Table S2), as previously described [57,58]. The relative expression levels (target miRNA/RNU6B) for each specific miRNA marker were assessed in each NCI and FaDu group treated with NNK and their untreated controls, by CFX96TM software (Bio-Rad).

2.7. Transfection of NCI and FaDu with Mimic/Inhibitor of miR-21

MicroRNA-21 mimic (miScript miRNA Mimic, Qiagen) or miR-21 inhibitor (Antihsa-miR-21-5p; Qiagen) (Supplementary Table S1) were diluted to a final concentration of 5 nM in serum-free culture medium, including HiPerFect[®] Transfection Reagent (3 μ L/well) (Qiagen), according to the manufacturers’ instructions, and incubated for 10 min at room temperature. Cells (NCI and FaDu) were mixed with transfected complexes, seeded at 1.5×10^5 cells/well of 24-well plates and incubated for 24 h under normal growth conditions (at 37 °C and 5% CO₂). The next day, the media were removed and replaced with experimental media of 1 μ M or 2 μ M NNK. Untreated control groups were grown in serum-free basal media, in parallel to experimental groups. After 24 h, media were removed, the cells were washed once with PBS and total protein was isolated using M-PER reagent (mammalian protein extraction reagent; Thermo Scientific).

Assays were carried out according to the manufacturer’s instructions and performed in triplicate. All experiments were independently repeated three times.

2.8. Enzyme-Linked Immunosorbent Assay for Total MSH2 Quantification

We performed a direct enzyme-linked immunosorbent assay (ELISA) to determine the total levels of MSH2 protein expression in NCI and FaDu treated with NNK and their untreated controls, with or without the presence of mimic miR-21 and miR-21 inhibitor. Total protein concentrations were determined using the BCA-200 Protein Assay kit (Thermo Scientific), and total MSH2 expression levels were determined by ELISA as follows:

Nunc MaxiSorpTM 96-well plates (Invitrogen by Thermo Fisher Scientific) were coated with 100 μ L of total protein extracts from NCI and FaDu, at a concentration of 10 μ g/mL, in 1X coating buffer [protein added to coating buffer and mixed for 15 min; 1X coating buffer diluted from 5X stock (BUF030A; BIORAD) in dH₂O and mixed for 15 min].

The plates were covered and incubated at 4 °C overnight. The next day, the plates were washed 3 times in wash buffer (PBST; 0.05% v/v Tween-20 in PBS), incubated in 150 μ L/well of blocking solution (1% w/v BSA in PBS) for 60 min at 37 °C, and then washed 4 times in wash buffer and incubated in 100 μ L/well of primary MSH2 (Clone D-6) mouse monoclonal antibody HRP (horseradish peroxidase) or β -actin (C4) mouse monoclonal antibody HRP (Santa Cruz Biotechnology), which was used as a reference control for protein normalization, for 1 h at 37 °C (we used 0.3 μ g of each antibody per 10 μ g of total protein; antibodies were diluted in 1%BSA/PBS). Finally, the plates were washed 3 times in wash buffer and incubated in 100 μ L/well of TMB Core+ substrate solution (3,3', 5, 5'-tetramethylbenzidine plus hydrogen peroxide) BUF062C; Bio-Rad) for 30 min at room temperature in the dark. We read the absorbance values immediately at 600 nm using a microplate reader (Sunergy1, BIOTEK; Gen5TM software, BioTek Instruments Inc., Winooski, VT, USA). Protein standards for both MSH2 and β -actin were used by 1:10 serial dilutions of a highly concentrated protein sample that was positive for MSH2.

Assays were carried out according to the manufacturer's instructions and performed in triplicate. All experiments were repeated three times, independently.

2.9. Cell Viability Assay

We performed a cell viability assay, using Cell Titer-Glo[®] Luminescent Cell Viability Assay (Promega Corp., Madison, WI, USA), to monitor the effect of 1 μ M and 2 μ M of NNK on NCI and FaDu treated cells, compared to their corresponding untreated controls. The cells were seeded at a density of 5000 cells/well in 24-well plates. The next day, the cells were exposed for 24 h to experimental media. At the end of the treatment, we removed the media and replaced them with serum-free basal media. Untreated controls were also grown in serum-free basal media. Cells were cultured at 37 °C in humidified air and 5% CO₂ for 3 days. We then used a luminometer to measure the luminescence. We determined the cell viability by comparing the mean values of cells exposed to NNK versus the mean values of untreated cells, for each cancer cell line. The statistically significant difference in cell viability was determined using paired-test and p -value < 0.05 (Graph Pad Prism 7.0, GraphPad Software Inc., San Diego, CA, USA). All experiments were repeated three times, independently.

2.10. Statistical Analysis

We used GraphPad Prism 7 software and multiple t -test analysis (GraphPad Prism 7 software; t -test; multiple comparisons by Holm-Sidak) to show the differential expression (p -values) for each analyzed gene and protein expression between different experimental and control groups. Pearson correlation was performed to estimate the correlation coefficient between the transcriptional levels of the analyzed MMR genes and the proteins, as well as between the expression levels of MMR genes or proteins and "oncomirs", in the different NCI and FaDu groups (p -values < 0.05).

3. Results

3.1. Either Low or High Dose of NNK Reduces MSH2 and MLH1 Protein Levels in Both LSCC and HSCC Cells

Immunocytochemical and western blot analyses revealed that exposure to either a low or high dose of NNK causes a significant decrease in the expression and nuclear translocation of mismatch DNA repair proteins, MSH2 and MLH1, in both NCI and FaDu treated cells, compared to untreated controls (Figure 1, Figure 2, and Figure 3).

Specifically, as depicted in Figure 2 by immunocytochemical analysis, both untreated NCI and FaDu cells showed strong nuclear MSH2 localization. In contrast, both NCI and FaDu exposed to either a low (1 μ M) or high (2 μ M) dose of NNK exhibited weak nuclear and/or cytoplasmic staining for MSH2 compared to untreated controls (Figure 1A-a,B-a). Scoring of MSH2 positivity revealed significantly lower MSH2 levels in NCI and FaDu exposed to either 1 μ M or 2 μ M of NNK, compared to untreated controls (Figure 1A-b,B-b) [p < 0.05, t -test; means (SD); multiple comparisons by Holm-Sidak].

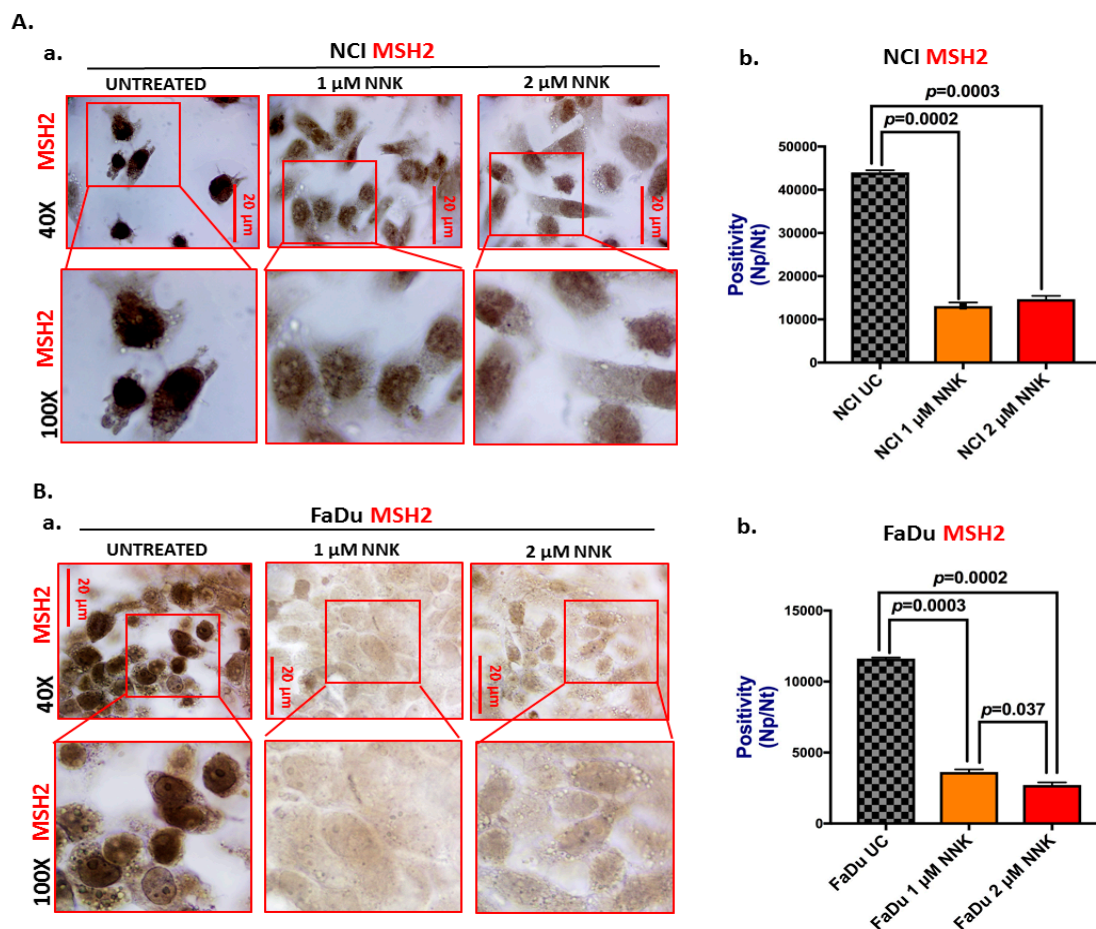


Figure 1. Either low or high dose of NNK reduces MSH2 expression in both lung (NCI) and head and neck (FaDu) cancer cells. Immunoperoxidase cell staining for MSH2 reveals that (A) NCI and (B) FaDu exposed to either 1 μ M or 2 μ M of NNK produce reduced MSH2 nuclear levels, as indicated by (A-a and B-a) the less intense MSH2 staining (scale bar: 20 μ m), and (A-b and B-b) the significantly lower nuclear MSH2 levels [Np/Nt = Number of nuclear positive/total number of nuclei, means(SD)], compared to untreated controls. Data were obtained from two independent images (≥ 10 cells) (p values by t -test; multiple comparisons by Holm-Sidak; GraphPad Prism 7.0). Images were captured using Aperio CS2 and analyzed by Image Scope software (Leica Microsystems, Buffalo Grove, IL).

Also, as depicted in Figure 2, by immunofluorescence assay, both untreated NCI and FaDu cells showed intense nuclear staining of MLH1. In contrast, both NCI and FaDu exposed to either a low (1 μ M) or high (2 μ M) dose of NNK exhibited weak staining for nuclear MLH1 (Figure 2A-a,B-a). Scoring of nuclear MLH1 revealed statistically significantly lower MLH1 levels in NCI and FaDu exposed to 1 μ M or 2 μ M of NNK, compared to untreated controls (Figure 2A-b,B-b) [$p < 0.05$, t -test; means (SD); multiple comparisons by Holm-Sidak]. Scoring of nuclear MLH1 also revealed statistically significantly lower MLH1 levels in FaDu exposed to 2 μ M compared to those exposed to 1 μ M of NNK.

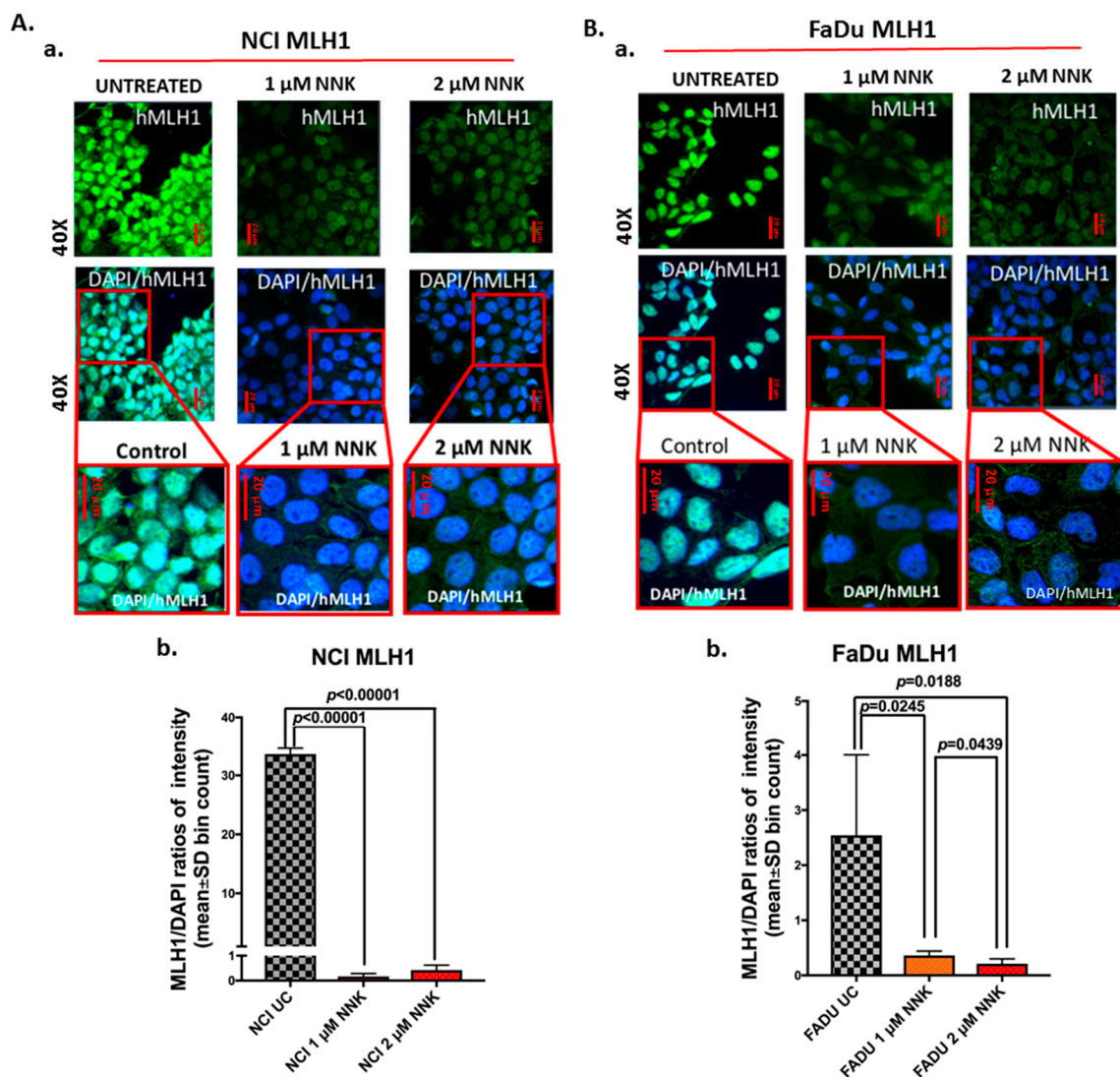


Figure 2. Either low or high dose of NNK reduce MLH1 expression in both lung (NCI) and head and neck (FaDu) cancer cells. Immunofluorescence staining for MLH1 reveals that (A) NCI and (B) FaDu exposed to either 1 μ M or 2 μ M of NNK produce reduced MLH1 nuclear levels, as indicated by (A-a and B-a) the weak nuclear staining of MLH1 (green: MLH1; blue: DAPI for nuclear staining; scale bar: 20 μ m), and (A-b and B-b) the significantly lower nuclear MLH1 levels [MLH1/DAPI means(SD) bin count, by Zen imaging software], compared to untreated controls. Data were obtained from four independent images (p values by t -test; multiple comparisons by Holm-Sidak; GraphPad Prism 7.0).

Western blot analysis confirmed the above immunohistochemical analysis data. Specifically, as shown in Figure 3, both NCI and FaDu exposed to a low (1 μ M) or high (2 μ M) dose of NNK showed significantly lower MSH2 and MLH1 nuclear translocation ratios (nuclear vs. cytoplasmic levels) (Figure 3A-a,B-a) compared to untreated controls. In general, the high NNK dose induced lower nuclear translocation ratios of MMR proteins compared to the low dose (Figure 3A-b,B-b). NCI exposed to either a low or high dose of NNK produced a similar reduction of MSH2 and MLH1. In general, total MMR (MSH2 and MLH1) protein levels were significantly reduced in NNK-treated NCI and FaDu, relative to their untreated controls (Supplementary Figure S1).

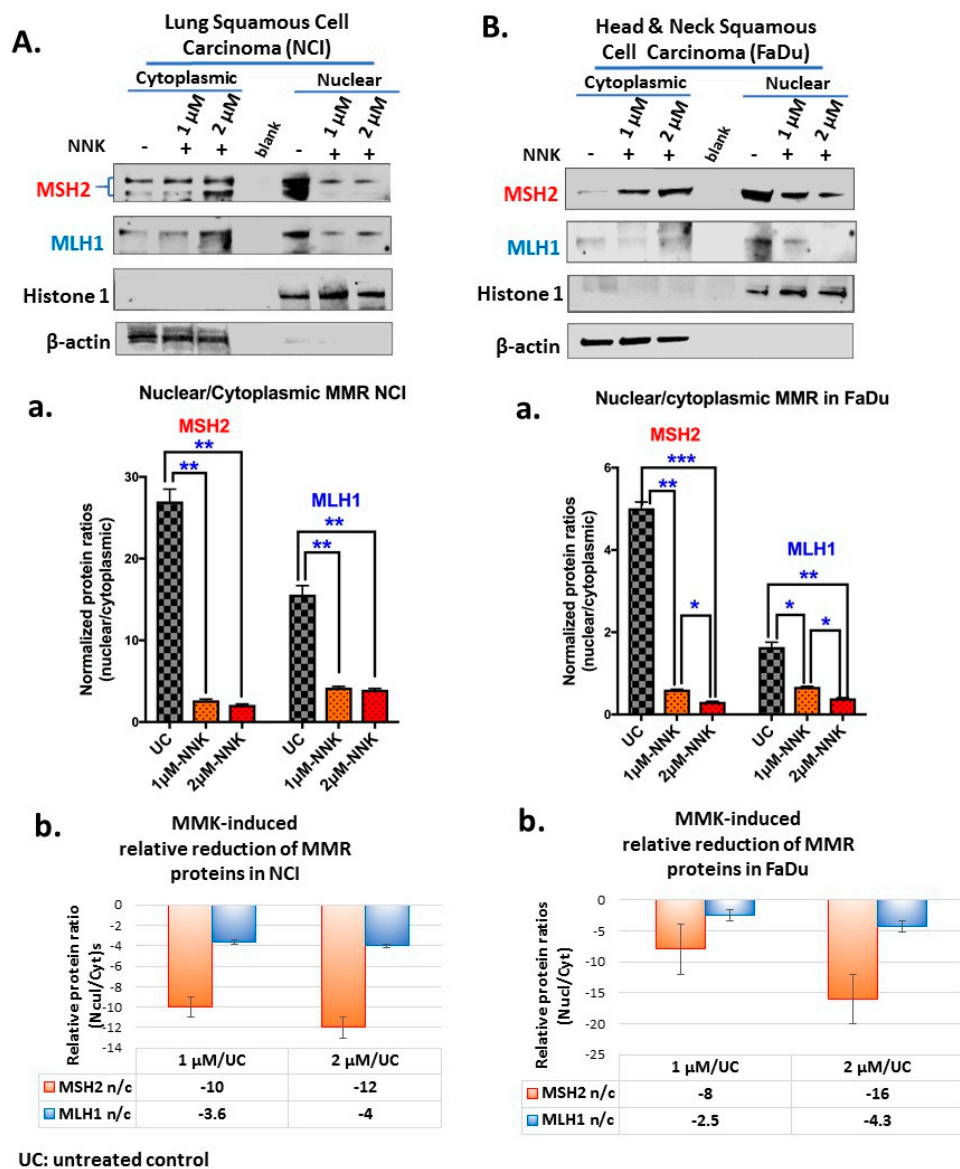


Figure 3. Either low or high dose of NNK reduces the nuclear translocation of MMR (MSH2 and MLH1) proteins in both (A) NCI and (B) FaDu cells. Graphs depict MSH2 and MLH1 nuclear translocation ratios (nuclear/cytoplasmic protein expression levels) (A-a and B-a), in NCI and FaDu cells, respectively, exposed to 1 μ M or 2 μ M of NNK compared to untreated controls. (A-b and B-b) NNK-induced relative reduction of MMR nuclear translocation in NCI and FaDu cells, respectively, is demonstrated by the relative MMR n/c (nuclear/cytoplasmic) protein ratios in NNK-treated vs. untreated controls. (β -actin and Histone 1 were used to normalize cytoplasmic and nuclear protein extracts, respectively, by western blot analysis; UC: untreated controls). [Paired *t*-test, * *p* < 0.05; ** *p* < 0.005; *** *p* < 0.0005; **** *p* < 0.00005; GraphPad Prism 7.0; means (SD) of three independent experiments].

3.2. Either Low or High Dose of NNK Reduces hMSH2 and hMLH1 mRNAs in Both LSCC and HSCC Cells

Gene expression analysis by quantitative PCR revealed that exposure to either a low or high dose of NNK induced a significant decrease in both *hMSH2* and *hMLH1* mRNAs in treated NCI and FaDu cell lines compared to untreated controls, as illustrated in Figure 4.

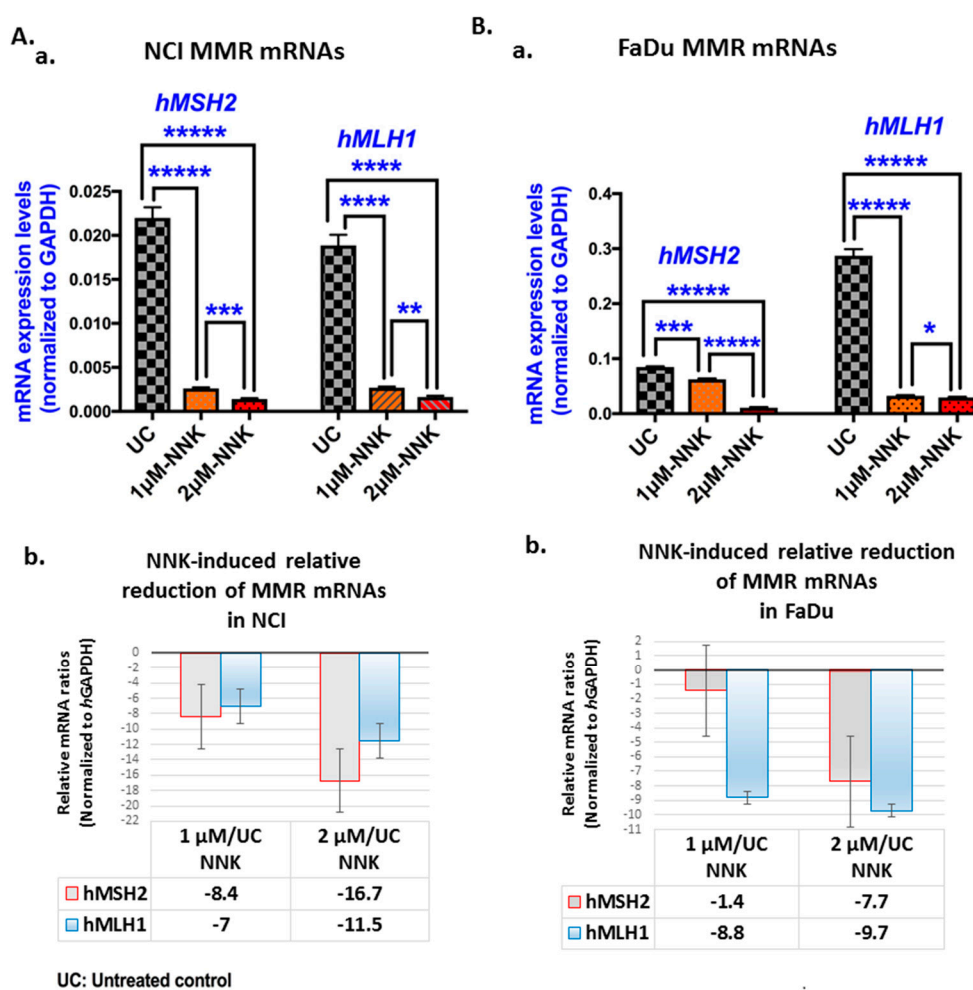


Figure 4. Either low or high dose of NNK reduces *hMSH2* and *hMLH1* mRNAs in both (A) NCI and (B) FaDu. (A-a and B-a) Graphs depict the transcriptional levels of the MMR genes, *hMSH2* and *hMLH1* (relative to *hGAPDH* reference gene) induced in untreated and NNK-treated NCI and FaDu. Data were obtained from real-time qPCR analysis. (Graphs, created by GraphPad Prism 7 software; *** $p < 0.0005$; **** $p < 0.0005$, ***** $p < 0.00005$; by *t*-test; multiple comparisons by Holm-Sidak). (A-b and B-b) The graphs illustrate the NNK-induced mRNA reduction, as demonstrated by the relative mRNA ratios of MMR genes (*hMSH2* and *hMLH1*) in NNK-treated (at 1 μ M and 2 μ M) NCI and FaDu, respectively, versus untreated controls. (Data were obtained from three independent experiments).

Specifically, we found that both NCI and FaDu exposed to 2 μ M of NNK produced significantly lower transcriptional levels of *hMSH2* and *hMLH1* compared to those exposed to 1 μ M (Figure 4A-a,B-a; Supplementary Table S3).

In general, the high dose of NNK caused a more pronounced decrease in MMR mRNAs compared to the low dose, especially for *hMSH2* (Figure 4A-b,B-b). As shown in Table 1, *hMSH2* showed a 2-fold and 5.7-fold decrease in its mRNAs, in NCI and FaDu cells, respectively, exposed to 2 μ M of NNK, as compared to those exposed to 1 μ M.

Pearson analysis revealed a significant positive correlation between NNK-induced *hMSH2* and *hMLH1* reduced mRNA levels in NCI ($r = 0.9999$, $p < 0.009$). A positive correlation was also found between NNK-induced *hMSH2* and *hMLH1* mRNAs in FaDu; however, this was not found to be statistically significant ($r = 0.74$).

Pearson analysis also revealed a significant positive correlation between NNK-induced depleted *hMSH2* mRNAs and MSH2 nuclear protein levels in NCI ($r = 0.9997$, $p = 0.0155$). Positive correlations

were also found between NNK-induced decreased *hMLH1* mRNAs and MLH1 nuclear protein levels in both NCI ($r = 0.9798$) and FaDu ($r = 0.9458$); however, these were not found to be statistically significant.

The above observations support a linear correlation between the two main components (MSH2 and MLH1) of the MMR mechanism in both NCI and FaDu and between the levels of mRNAs and proteins of each MMR component in upper-aerodigestive tract cancer cells under NNK exposure.

Table 1. MMR mRNA and miRNA expression changes produced in Lung (NCI) and Head and Neck (FaDu) cancer cells exposed to high (2 μ M) versus to low (1 μ M) dose of NNK.

Upper Aero-Digestive Tract Cancer Cell Lines	*2 μ M vs. 1 μ M of NNK
Lung cancer cells (NCI)	
MMR genes	
<i>hMSH2</i>	2.0 ↓
<i>hMLH1</i>	1.6 ↓
miRNAs	
<i>miR-155</i>	2.5 ↑
<i>miR-21</i>	2.0 ↑
<i>miR-422a</i>	1.8 ↓
Head and Neck cancer cells (FaDu)	
MMR genes	
<i>hMSH2</i>	5.7 ↓
<i>hMLH1</i>	1.1 ↓
miRNAs	
<i>miR-155</i>	1.1 ↑
<i>miR-21</i>	1.8 ↑
<i>miR-422a</i>	1.0

* Fold-changes in normalized mRNA and miRNA levels (↓: decrease; ↑: increase)

3.3. NNK Induces Deregulation of “Oncomirs” *miR-21* and *miR-155*, and “Tumor Suppressor” *miR-422a*, in Exposed LSCC and HSCC Cells

MicroRNA analysis revealed that either a low or high dose of NNK can upregulate the “oncomirs”, *miR-155* and *miR-21* (Figure 5A,B), and downregulate the “tumor suppressor” *miR-422a* (Figure 5C,D) in NCI and FaDu, respectively.

We found that both NCI and FaDu exposed to 2 μ M of NNK produced significantly higher *miR-21* and *miR-155* levels compared to cells exposed to 1 μ M (Figure 5A-a,B-a). We also found that NCI exposed to 2 μ M of NNK produced significantly lower levels of *miR-422a* compared to those exposed to 1 μ M (Figure 5C-a,D-a) (Supplementary Table S4).

In general, the high dose of NNK caused a more profound upregulation of the analyzed “oncomirs” compared to the low dose, especially for *miR-21*, in both NCI and FaDu (Figure 5A-b,B-b). As shown in Table 1, *miR-21* showed a 1.8-fold and 2.0-fold increase in NCI and FaDu, respectively, and *miR-155* showed a 2.5-fold increase in NCI exposed to 2 μ M of NNK compared to those exposed to 1 μ M. On the other hand, the high dose of NNK induced a more profound downregulation of *miR-422a* than the low dose, in NCI (Figure 5C-b), by a 1.8-fold decrease (2 μ M vs. 1 μ M of NNK), as shown in Table 1. However, a similar downregulation of *miR-422a* was found in FaDu exposed to either a low (1 μ M) or high (2 μ M) dose of NNK (Figure 5D-b).

A Pearson analysis revealed (i) a linear correlation between the levels of *miR-21* and *miR-155* induced by NNK in both NCI ($r = 0.9393$) and FaDu ($r = 0.9540$), and (ii) an inverse correlation between the levels of *miR-155* and *miR-422a* induced by NNK in both NCI ($r = -0.9806$) and FaDu ($r = -0.9962$), although this was not found to be statistically significant.

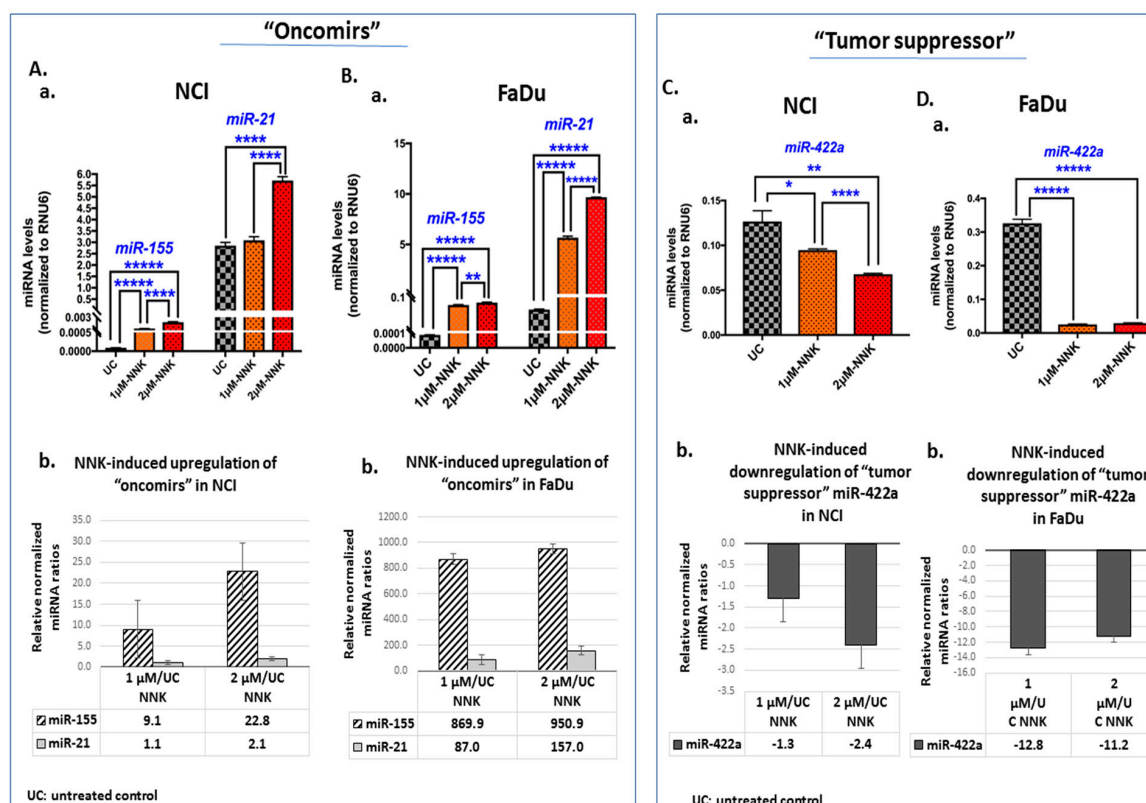


Figure 5. Either low or high dose of NNK induces deregulation of “oncomirs”, miR-21 and miR-155, and “tumor suppressor” miR-422a, in (A) NCI and (B) FaDu. (A-a and B-a) Graphs depict the expression levels of “oncomirs”, miR-155 and miR-21, in untreated and NNK-treated NCI and FaDu, respectively. (A-b and B-b) The graphs illustrate the NNK-induced upregulation of “oncomirs”, miR-21 and miR-155, in NCI and FaDu cells, respectively, as demonstrated by the relative expression ratios in NNK-treated (1 μ M or 2 μ M) versus untreated controls. (C-a and D-a) The graphs illustrate the NNK-induced downregulation of “tumor suppressor” miR-422a, in NCI and FaDu, respectively, as demonstrated by the relative expression ratios in NNK-treated (1 μ M or 2 μ M) versus untreated controls. [miRNA levels were normalized to RNU6 reference control. Data were obtained from three independent experiments; p values by t -test; * $p < 0.05$, ** $p < 0.005$, **** $p < 0.00005$, ***** $p < 0.000005$; GraphPad Prism 7.0, means (SD)].

3.4. Inhibition of miR-21 prevents NNK-induced MSH2 reduction

We used a mimic miR-21 and an inhibitor of miR-21 to mechanically analyze their effect on NNK-induced suppression of total MSH2 protein levels. Elisa revealed that inhibition of miR-21 prevents the reduced MSH2 phenotype induced by NNK in NCI and FaDu treated cells (Figure 6).

We observed that either a low (1 μ M) or high (2 μ M) dose of NNK caused a significant decrease in total MSH2 protein levels, in both NCI and FaDu treated cells compared to untreated controls. However, inhibition of miR-21 prevented the NNK-induced MSH2 depletion in treated cells (Figure 6, Supplementary Table S5). Specifically, at either low or high doses of NNK, both NCI and FaDu with inhibited miR-21, produced significantly higher levels of MSH2 protein compared to those without miR-21 inhibition. The observation that exposure to a high dose of NNK resulted in a significantly higher MMR expression in cells with inhibited miR-21 compared to untreated controls is probably due to the increased need for DNA repair under the harmful effect of NNK.

The suppressive effect of miR-21 on MSH2 protein levels was demonstrated by the observation that the mimic miR-21 induced significantly lower total MSH2 levels in both NCI and FaDu treated cells than untreated controls.

miR21-inh induced total MSH2

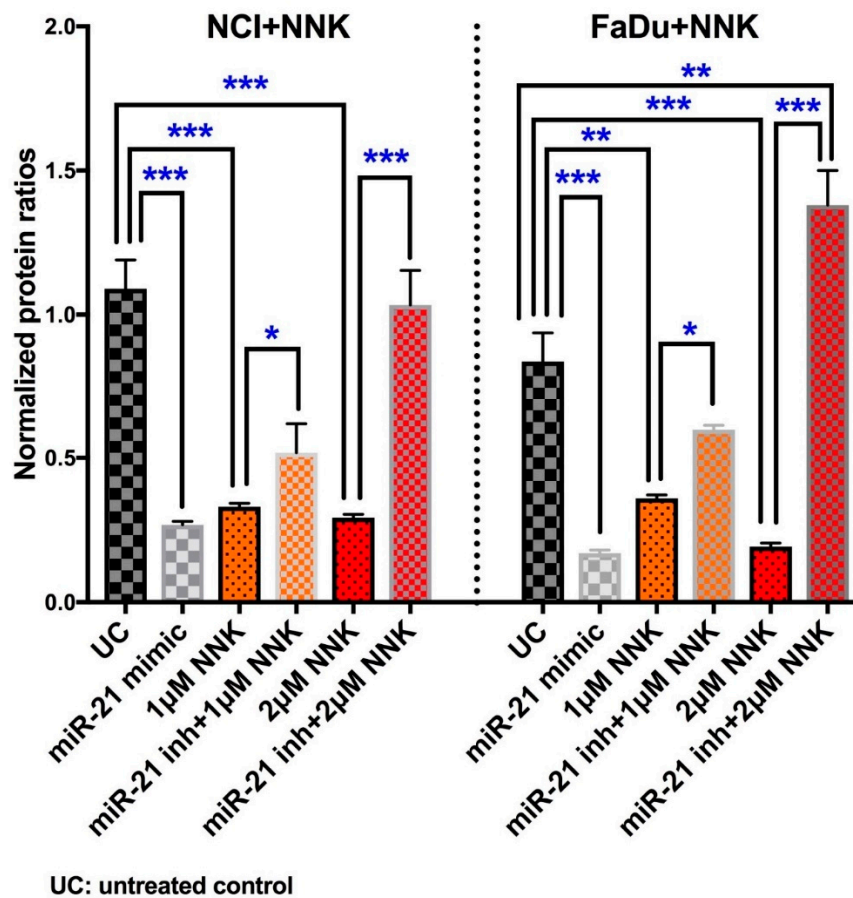


Figure 6. Inhibition of miR-21 prevents NNK-induced MSH2 reduction. Graphs created by GraphPad Prism 7.0 depict total MSH2 protein level in NCI and FaDu exposed to 1 μ M or 2 μ M of NNK, with and without miR-21 inhibitor. Controls: cells treated with mimic miR-21 and untreated controls. (Data obtained from three independent experiments [$* p < 0.05$; $** p < 0.005$; $*** p < 0.0005$, by *t*-test; multiple comparisons by Holm-Sidak; GraphPad Prism 7.0; means (SD)].

3.5. NNK Increases LSCC and HSCC Cell Viability that Can Be Prevented by miR-21 Inhibition

NNK increased cell viability in both NCI and FaDu treated cells compared to untreated controls (Figure 7A).

In particular, NCI exposed to 1 μ M or 2 μ M of NNK exhibited a similar increase in cell viability compared to untreated controls (Figure 7A). Although FaDu exposed to both 1 μ M and 2 μ M of NNK increased cell viability compared to untreated controls, it appeared that 2 μ M of NNK induced significantly higher survival rates compared to 1 μ M, in FaDu (Figure 7B).

The contribution of miR-21 in NNK-induced cell viability of NCI and FaDu cells was explored by the application of miR-21 inhibitor. As shown in Figure 7C,D, the application of miR-21 inhibitor produced a significant reduction in cell viability of NNK-treated NCI and FaDu, respectively ($p < 0.0005$).

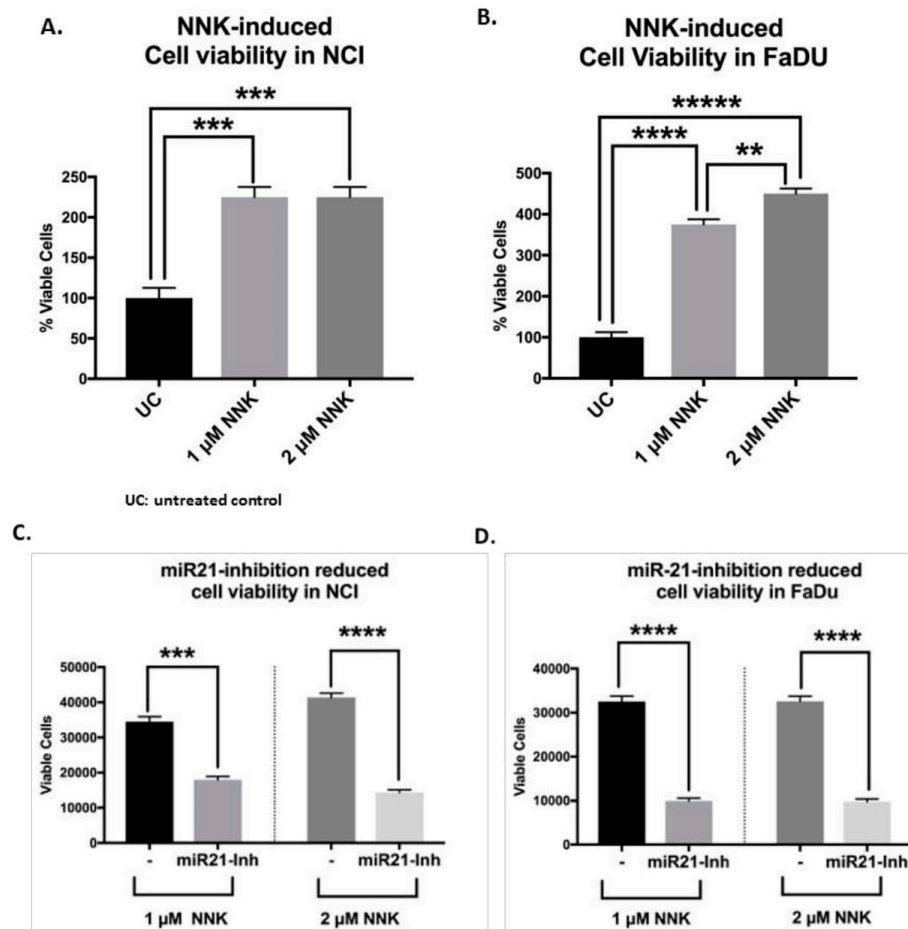


Figure 7. NNK promotes cell viability in lung (NCI) and head and neck (FaDu) squamous cancer cells, which is prevented by miR-21 inhibition. Graphs depict the viability rates in (A) NCI and (B) FaDu exposed to 1 μ M and 2 μ M of NNK (% of viable cells in NNK groups vs untreated controls) and the changes in the viability of (C) NCI and (D) FaDu cells under the inhibition of miR-21 (miR21-inh). Graphs, created by GraphPad Prism 7 software; ** $p < 0.005$; *** $p < 0.0005$; **** $p < 0.00005$; ***** $p < 0.000005$, by t -test; multiple comparisons by Holm-Sidak. (Data are derived from three independent experiments.).

3.6. LSCC Versus HSCC under NNK Exposure

NNK induced a more profound effect on miR-21, miR-155 and miR-422a deregulation in HSCC (FaDu) compared to LSCC (NCI) cells, either at a low or high dose. On the other hand, NNK induced a more profound effect on MMR genes downregulation in LSCC compared to HSCC cells, especially at a high dose (Figure 4A-b,B-c).

However, NNK produced a reduced MMR phenotype and miRNA deregulations in both LSCC and HSCC cells. In addition, miR-21 inhibition prevented NNK-induced MSH2 reduction in both LSCC and HSCC cells.

4. Discussion

Tobacco smoke is an established risk factor of lung and head and neck cancers [61,62], and is considered to contribute to their recurrence and progression [63,64]. There is evidence that patients with head and neck squamous cell carcinoma often develop primary squamous cell lung carcinoma [65]. This suggests that common mechanisms may apply in both types of cancer [66]. Here, we demonstrate that tobacco smoke carcinogen, NNK, can affect the expression of cancer-related miR-21, miR-155 and miR-422a, which have a regulatory role in the MMR mechanism, causing downregulation of

hMSH2 and *hMLH1*, and increase cell survival in both lung and head and neck squamous cancer cells (Figure 8A).

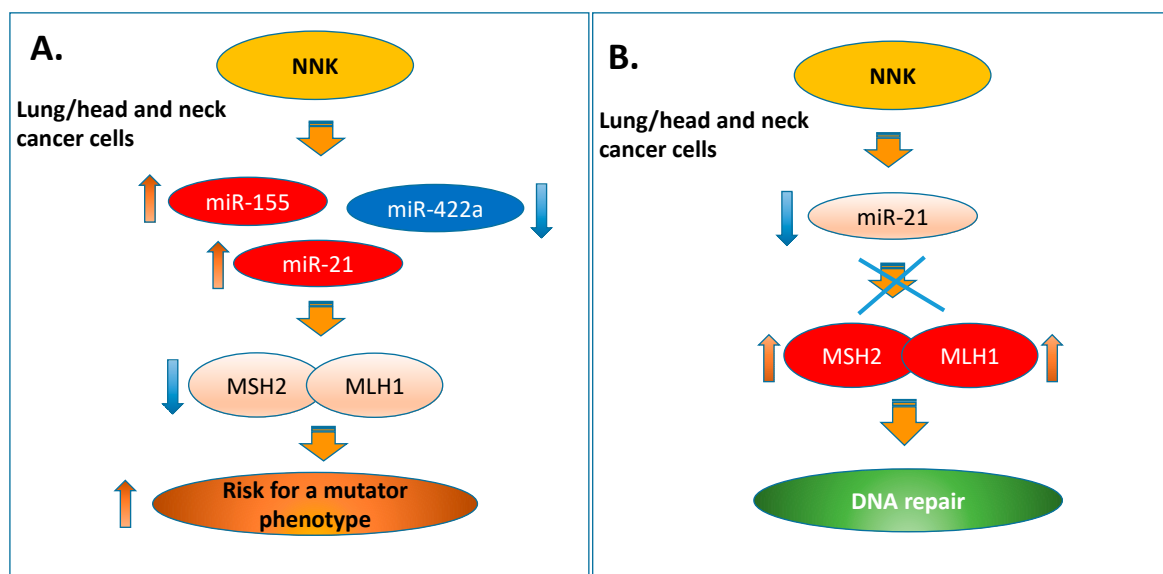


Figure 8. NNK-induced deregulation of miRNA and Mismatch DNA repair expression profiles in lung and head and neck squamous cancer cells. Schematic presentation of (A) the proposed mechanism by which NNK induced deregulation of miRNA and MMR genes increasing the risk for a mutator phenotype in lung and head and neck squamous cancer cells (B) the proposed preventive effect of miR-21 inhibition in this process.

In general, the deregulation of microRNA expression has been associated with gene alterations that are commonly linked to smoke-related cancers [67–69]. The “oncomirs” miR-21 and miR-155 have previously been associated with cancers of the upper aerodigestive tract [48,49,51–54]. In particular, miR-21 has been considered as a marker of poor prognosis in lung and head and neck cancer [70,71]. To our knowledge, we are the first to present an association between the NNK effect and miR-21, miR-155 and miR-422a deregulations in lung and head and neck squamous cancer cells, supporting them as possible biomarkers in NNK-induced gene alterations.

In principle, miRNAs are involved in the regulation of numerous genes related to various physiological processes, including MMR genes [38–46,72]. As we previously discussed, miR-155 and miR-422a are known to be involved in MMR mechanism regulation [43,46]. Although miRNA-21 is a crucial factor for both types of malignancies, there is limited literature regarding the involvement of miR-21 in the MMR mechanism [39–42]. Here, our novel findings have shown that the NNK-induced upregulation of “oncomir” miR-21 directly affects MSH2 protein levels in both lung and head and neck squamous cancer cells, and that its inhibition can restore the MSH2 expression phenotype (Figure 8B). These findings document the regulatory role of miR-21 in the MMR mechanism by directly affecting MSH2, which is a key component of the MutSa complex that recognizes base–base mismatches and short insertion and deletion loops [24]. We also showed that inhibition of miR-21 significantly decreases NNK-induced cell survival. Although multiple mechanisms could be involved in this process, our data suggest that the miR-21 could possibly play an important role in NNK-induced antiapoptotic effect. This is consistent with previous report suggesting that miR-21 is directly involved in cell cycle regulation by inhibiting MSH2 [42].

NNK is one of the tobacco products that has been evaluated by the International Agency for Research on Cancer (IARC) [73]. Evidence of NNK carcinogenicity was provided by preclinical studies [62]. NNK can be metabolically activated to intermediates that react with DNA forming covalently-bound products known as adducts. The NNK-mediated formation of DNA adducts is crucial to the carcinogenic process [74]. The defect in the DNA repair mechanism leads to mutation

due to unrepaired NNK-induced DNA adducts. Although damaged or mutated DNA can be removed by apoptosis, cell survival due to either upregulation of the antiapoptotic mechanism or mutations that occur in cancer-related regions may result in uncontrolled cellular growth (antiapoptotic process) and tumor development. Previous experimental studies provided evidence that MMR deficiency is associated with tumor progression [75]. Our data showed that NNK, especially at a high dose, in parallel to inducing MMR deregulation, also promotes the cellular viability of NCI and FaDu. Clearly, promoting the antiapoptosis in a cell with a defective DNA repair mechanism increases the risk for a mutator phenotype (Figure 8A), and potentially increases the risk for malignant progression.

The role of NNK-induced tumorigenicity appeared to be complex. Earlier studies have shown that NNK-induced decreased binding of the nucleotide excision repair (NER) proteins XPA and XPB to DNA could be responsible for the decrease in repair activities in lung [76,77]. This observation supports the hypothesis that NNK can not only alter the level of MMR proteins, but may, in parallel, affect modifications of NER proteins, resulting in defective DNA repair. It is believed that NNK can affect the level of proteins related to DNA repair mechanisms by inducing the formation of pyridyloxobutyl and methyl adducts [77]. Specifically, NNK-induced DNA methylation, like promoter hyper-methylation of MLH1 and MSH2 [78,79], can significantly affect the ability of cells to repair genetic damage [80]. Therefore, the observed NNK-induced alterations of the MMR gene expression presented here cannot rule out their epigenetic regulation through the NNK-induced DNA methylation. However, NNK-induced DNA methylation can, at the same time, modulate miRNA levels by regulating MMR gene expression. Hypo- or hyper- methylation of miRNA was considered to represent a new level of complexity in gene regulation in human cancers [81], suggesting miR-21 or miR-155 promoter hypo-methylation [81–84] and miR-422a hyper-methylation, as previously reported for miR-373 [81,85], as potential epigenetic modifications caused by tobacco carcinogenic effects on MMR. On the other hand, alkylating agents, such as NNK can also directly or after biological activation react and form covalent bonds with nucleophilic centers found in DNA and RNA and proteins [86], supporting possible direct interference of NNK with levels of miRNAs, thereby causing their deregulation [48,49,51–54]. Subsequently, NNK-induced miRNA deregulations can affect MMR gene expression, either through post-transcriptional modifications or through DNA methylation by targeting DNA methyltransferases or methylation-related proteins [81].

Our novel findings showed that either a low or high NNK dose can cause a significant upregulation of “oncomirs” miR-21 and miR-155 and downregulation of “tumor suppressor” miR-422a, as well as a decrease in *hMSH2* and *hMLH1* at both transcriptional and protein expression levels in exposed lung and head and neck squamous cancer cells. Although further exploration of a possible dose-dependent effect of NNK on the MMR mechanism is required, our study showed that a higher NNK dose induces a more extended effect on miRNA, particularly on miR-155 and miR-422a, and MMR expression compared to lower doses. On the other hand, the fact that even a low dose of NNK was capable of causing significant alterations in MMR and miRNA expression indicates that even a small exposure to the tobacco smoke carcinogen could have potentially harmful consequences. Taking into consideration the theory that long-term exposure to chemicals, even at low doses, could have an augmented effect [87,88], long-term studies could reveal the chronic effect of low NNK exposure to MMR genes in lung and head and neck squamous cancer cells.

It is thought that high levels of MMR can positively contribute to the efficacy of chemotherapy [89,90], while a significant number of preclinical and clinical data have shown that inactivation of *hMLH1* and *hMSH2* promotes resistance to cisplatin and carboplatin-based chemotherapy [34,35]. According to previous findings from our group, a defective MMR phenotype is not beneficial for cisplatin chemotherapy, resulting in low survival rates in patients with lung squamous cell carcinoma [34]. Recently, there has been increasing interest in assessing the predictive value of a defective MMR mechanism in various types of cancer, including lung and head and neck cancer [91,92]. In addition, recent studies strongly support that MMR status can alter the efficacy of target immunotherapy, and the identification of MMR status prior to initiation of treatment may be a useful approach [36,83]. The fact

that NNK, in addition to its mutagenic effect, which is manifested by inducing DNA defects, can simultaneously suppress the DNA repair mechanism and promote cellular antiapoptosis, supports its carcinogenic potency. Our observation that NNK caused a decrease in the expression of MMR genes in lung and head and neck squamous cancer cells may support the theory that exposure of these cells to tobacco smoke could have a potential modulatory effect in the treatment and natural history of the disease.

5. Conclusions

In summary, the current study shows that NNK, either at a high or low dose, can cause deregulation in miR-21, miR-155 and miR-422a, and downregulation of MMR genes. In addition to promoting the deregulation of the MMR mechanism, NNK can simultaneously enhance the viability of cancer cells, potentially promoting cancer progression. Finally, inhibition of miR-21 can restore NNK-induced MSH2 reduction and decreases cell survival.

All the above provide further information on the effects of NNK on cancer development and progression, and give insights into the impact that smoke-carcinogens could have on the MMR status. Further studies should reveal the utility of MMR genes and miRNAs as diagnostic biomarkers and as a tool for novel diagnostic and therapeutic approaches in lung and head and neck squamous cell carcinomas.

Supplementary Materials: The data supports the findings of this study are available in the supplementary material of this article at <http://www.mdpi.com/2073-4409/9/4/1031/s1> (Table S1: Human genes analyzed by real-time qPCR, in human lung (NCI) and head and neck (FaDu) cancer cells; Table S2: Human miRNAs and small RNA analyzed by real-time qPCR, in human lung (NCI) and head and neck (FaDu) cancer cells; Table S3: Transcriptional levels of MMR genes in human lung (NCI) and head and neck (FaDu) cancer cells (by qPCR); Table S4: Expression levels of miRNA specific markers analyzed in human lung (NCI) and head and neck (FaDu) cancer cells (by qPCR); Table S5: Total MSH2 protein level in NCI and FaDu exposed to 1 μ M or 2 μ M of NNK, with and without miR-21 inhibitor and Figure S1: Total MMR protein levels in NNK treated NCI and FaDu.

Author Contributions: Conceptualization, S.G.D., D.P.V., and A.T.; Methodology, D.P.V., and S.G.D.; Software, S.G.D., and D.P.V.; Formal Analysis, S.G.D., and D.P.V.; Investigation, S.G.D. and D.P.V.; Validation, S.G.D., D.P.V., G.L., D.A.S., C.T.S., and A.T.; Resources, D.P.V., and C.T.S.; Data curation, S.G.D. and D.P.V.; Writing-draft preparation, S.G.D. and D.P.V.; Writing-review and editing, S.G.D., D.P.V., G.L., D.A.S., C.T.S., and A.T.; Visualization, S.G.D. and D.P.V.; Supervision, S.G.D. and D.P.V., and A.T.; Funding acquisition, C.T.S. and A.T. All authors have read and agreed to the published version of the manuscript.

Funding: This study was supported by the Virginia Alden Wright Fund and partially supported by ELKE grants of Toxicology Lab University of Crete.

Conflicts of Interest: The authors declare no conflict of interest.

References

1. Sasco, A.J.; Secretan, M.B.; Straif, K. Tobacco smoking and cancer: A brief review of recent epidemiological evidence. *Lung Cancer* **2004**, *45*, S3–S9. [[CrossRef](#)] [[PubMed](#)]
2. Centers for Disease Control and Prevention (US); National Center for Chronic Disease Prevention and Health Promotion (US); Office on Smoking and Health (US). *How Tobacco Smoke Causes Disease: The Biology and Behavioral Basis for Smoking-Attributable Disease: A Report of the Surgeon General*; Centers for Disease Control and Prevention (US): Atlanta, GA, USA, 2010.
3. Islami, F.; Torre, L.A.; Jemal, A. Global trends of lung cancer mortality and smoking prevalence. *Transl. Lung Cancer Res.* **2015**, *4*, 327–338. [[CrossRef](#)] [[PubMed](#)]
4. Vardavas, C.I.; Bécuwe, N.; Demjén, T.; Fernández, E.; McNeill, A.; Mons, U.; Tountas, Y.; Trofor, A.C.; Tsatsakis, A.; Rohde, G.; et al. Study Protocol of European Regulatory Science on Tobacco (EUREST-PLUS): Policy implementation to reduce lung disease. *Tob. Induc. Dis.* **2018**, *16*, 2. [[CrossRef](#)]
5. Tsitsimpikou, C.; Tsarouhas, K.; Vasilaki, F.; Papalexis, P.; Dryllis, G.; Choursalas, A.; Spandidos, D.A.; Tsatsakis, A.; Charvalos, E.; Bacopoulou, F. Health risk behaviors among high school and university adolescent students. *Exp. Med.* **2018**, *16*, 3433–3438. [[CrossRef](#)] [[PubMed](#)]

6. Centers for Disease Control and prevention. Available online: <https://www.cdc.gov/media/releases/2016/p1110-vital-signs-cancer-tobacco.html> (accessed on 10 November 2016).
7. De Groot, P.M.; Wu, C.C.; Carter, B.W.; Munden, R.F. The epidemiology of lung cancer. *Transl. Lung Cancer Res.* **2018**, *7*, 220–233. [[CrossRef](#)]
8. Cohen, N.; Fedewa, S.; Chen, A.Y. Epidemiology and Demographics of the Head and Neck Cancer Population. *Oral Maxillofac. Surg. Clin. North Am.* **2018**, *30*, 381–395. [[CrossRef](#)]
9. American Cancer Society. Laryngeal and Hypopharyngeal Cancer 2019. Available online: <https://www.cancer.org/cancer/laryngeal-and-hypopharyngeal-cancer/detection-diagnosis-staging/survival-rates.html> (accessed on 9 January 2020).
10. Pfeifer, G.P.; Denissenko, M.F.; Olivier, M.; Tretyakova, N.; Hecht, S.S.; Hainaut, P. Tobacco smoke carcinogens, DNA damage and p53 mutations in smoking-associated cancers. *Oncogene* **2002**, *21*, 7435–7451. [[CrossRef](#)]
11. Zhong, Y.; Carmella, S.G.; Upadhyaya, P.; Hochalter, J.B.; Rauch, D.; Oliver, A.; Jensen, J.; Hatsukami, D.; Wang, J.; Zimmerman, C.; et al. Immediate consequences of cigarette smoking: Rapid formation of polycyclic aromatic hydrocarbon diol epoxides. *Chem. Res. Toxicol.* **2011**, *24*, 246–252. [[CrossRef](#)]
12. Boda, D.; Docea, A.O.; Calina, D.; Ilie, M.A.; Caruntu, C.; Zurac, S.; Neagu, M.; Constantin, C.; Branisteanu, D.E.; Voiculescu, V.; et al. Human papilloma virus: Apprehending the link with carcinogenesis and unveiling new research avenues (Review). *Int. J. Oncol.* **2018**, *52*, 637–655. [[CrossRef](#)]
13. Dylawerska, A.; Barczak, W.; Wegner, A.; Golusinski, W.; Suchorska, W.M. Association of DNA repair genes polymorphisms and mutations with increased risk of head and neck cancer: A review. *Med. Oncol.* **2017**, *34*, 197. [[CrossRef](#)]
14. Xue, J.; Yang, S.; Seng, S. Mechanisms of Cancer Induction by Tobacco-Specific NNK and NNN. *Cancers* **2014**, *6*, 1138–1156. [[CrossRef](#)] [[PubMed](#)]
15. Rohrer, J.; Wuertz, B.R.; Ondrey, F. Cigarette smoke condensate induces nuclear factor kappa-b activity and proangiogenic growth factors in aerodigestive cells. *Laryngoscope* **2010**, *120*, 1609–1613. [[CrossRef](#)] [[PubMed](#)]
16. Swenson, W.G.; Wuertz, B.R.; Ondrey, F.G. Tobacco carcinogen mediated up-regulation of AP-1 dependent pro-angiogenic cytokines in head and neck carcinogenesis. *Mol. Carcinog.* **2011**, *50*, 668–679. [[CrossRef](#)] [[PubMed](#)]
17. Hirata, N.; Yamada, S.; Sekino, Y.; Kanda, Y. Tobacco nitrosamine NNK increases ALDH-positive cells via ROS-Wnt signaling pathway in A549 human lung cancer cells. *J. Toxicol. Sci.* **2017**, *42*, 193–204. [[CrossRef](#)] [[PubMed](#)]
18. Zamay, T.N.; Zamay, G.S.; Kolovskaya, O.S.; Zukov, R.A.; Petrova, M.M.; Gargaun, A.; Berezovski, M.V.; Kichkailo, A.S. Current and Prospective Protein Biomarkers of Lung Cancer. *Cancers* **2017**, *9*, 155. [[CrossRef](#)]
19. Dahiya, K.; Dhankhar, R. Updated overview of current biomarkers in head and neck carcinoma. *World J. Methodol.* **2016**, *6*, 77–86. [[CrossRef](#)]
20. Tomasetti, C.; Marchionni, L.; Nowak, M.A.; Parmigiani, G.; Vogelstein, B. Only three driver gene mutations for cancer. *Proc. Nat. Aca. Sci. USA* **2015**, *112*, 118–123. [[CrossRef](#)]
21. Nogueira, G.A.; Lourenço, G.J.; Oliveira, C.B.; Marson, F.A.; Lopes-Aguiar, L.; Costa, E.F.; Lima, T.R.; Liutti, V.T.; Leal, F.; Santos, V.C.; et al. Association between genetic polymorphisms in DNA mismatch repair-related genes with risk and prognosis of head and neck squamous cell carcinoma. *Int. J. Cancer* **2015**, *137*, 810–818. [[CrossRef](#)]
22. Zienolddiny, S.; Ryberg, D.; Arab, M.O.; Skaug, V.; Haugen, A. Loss of heterozygosity is related to p53 mutations and smoking in lung cancer. *Br. J. Cancer* **2001**, *84*, 226–231. [[CrossRef](#)]
23. Vageli, D.; Daniil, Z.; Dahabreh, J.; Karagianni, E.; Vamvakopoulou, D.N.; Ioannou, M.G.; Scarpinato, K.; Vamvakopoulos, N.C.; Gourgoulialis, K.I.; Koukoulis, G.K. Phenotypic mismatch repair hMSH2 and hMLH1 gene expression profiles in primary non-small cell lung carcinomas. *Lung Cancer* **2009**, *64*, 282–288. [[CrossRef](#)]
24. Doukas, S.G.; Vageli, D.P.; Nikolouzakis, T.K.; Falzone, L.; Docea, A.O.; Lazopoulos, G.; Kalbakis, K.; Tsatsakis, A. Role of DNA mismatch repair genes in lung and head and neck cancer (Review). *World Acad. Sci. J.* **2019**, *1*, 184–191. [[CrossRef](#)]
25. Vageli, D.P.; Giannopoulos, S.; Doukas, S.G.; Kalaitzis, C.; Giannakopoulos, S.; Giatromanolaki, A.; Koukoulis, G.K.; Touloupidis, S. Mismatch repair hMSH2, hMLH1, hMSH6 and hPMS2 mRNA expression profiles in precancerous and cancerous urothelium. *Oncol. Lett.* **2013**, *5*, 283–294. [[CrossRef](#)] [[PubMed](#)]

26. Vageli, D.P.; Papamichali, R.; Kambosioras, K.; Papandreou, C.N.; Koukoulis, G.K. Mismatch DNA Repair hMSH2, hMLH1, hMSH6 and hPMS2 mRNA Expression Profiles in Colorectal Carcinomas. *J. Genet. Syndr. Gene Ther.* **2013**, *4*, 10.
27. Shia, J.; Ellis, N.A.; Klimstra, D.S. The utility of immunohistochemical detection of DNA mismatch repair gene proteins. *Virchows Arch.* **2004**, *445*, 431–441. [[CrossRef](#)] [[PubMed](#)]
28. Pereira, C.S.; Oliveira, M.V.; Barros, L.O.; Bandeira, G.A.; Santo, S.H.; Basile, J.R.; Guimarães, A.L.; De Paula, A.M. Low expression of MSH2 DNA repair protein is associated with poor prognosis in head and neck squamous cell carcinoma. *J. Appl. Oral Sci.* **2013**, *21*, 416–421. [[CrossRef](#)]
29. Demokan, S.; Suoglu, Y.; Demir, D.; Gozeler, M.; Dalay, N. Microsatellite instability and methylation of the DNA mismatch repair genes in head and neck cancer. *Ann. Oncol.* **2006**, *17*, 995–999. [[CrossRef](#)]
30. Wang, Y.; Irish, J.; MacMillan, C.; Brown, D.; Xuan, Y.; Boyington, C.; Gullane, P.; Kamel-Reid, S. High frequency of microsatellite instability in young patients with head-and-neck squamous-cell carcinoma: Lack of involvement of the mismatch repair genes hMLH1 and hMSH2. *Int. J. Cancer* **2001**, *93*, 353–360. [[CrossRef](#)]
31. Liu, K.; Huang, H.; Mukunyadzi, P.; Suen, J.Y.; Hanna, E.; Fan, C.Y. Promoter hypermethylation: An important epigenetic mechanism for hMLH1 gene inactivation in head and neck squamous cell carcinoma. *Otolaryngol. Head Neck Surg.* **2002**, *126*, 258–553. [[CrossRef](#)]
32. Hsu, H.S.; Wen, C.K.; Tang, Y.A.; Lin, R.K.; Li, W.Y.; Hsu, W.H.; Wang, Y.C. Promoter hypermethylation is the predominant mechanism in hMLH1 and hMSH2 deregulation and is a poor prognostic factor in nonsmoking lung cancer. *Clin. Cancer Res.* **2005**, *11*, 5410–5416. [[CrossRef](#)]
33. Scartozzi, M.; Franciosi, V.; Campanini, N.; Benedetti, G.; Barbieri, F.; Rossi, G.; Berardi, R.; Camisa, R.; Silva, R.R.; Santinelli, A.; et al. Mismatch repair system (MMR) status correlates with response and survival in non-small cell lung cancer (NSCLC) patients. *Lung Cancer* **2006**, *53*, 103–109. [[CrossRef](#)]
34. Vageli, D.P.; Zaravinos, A.; Daniil, Z.; Dahabreh, J.; Doukas, S.G.; Spandidos, D.A.; Gourgoulisanis, K.I.; Koukoulis, G.K. hMSH2 and hMLH1 gene expression patterns differ between lung adenocarcinoma and squamous cell carcinoma: Correlation with patient survival and response to adjuvant chemotherapy treatment. *Int. J. Biol. Markers* **2013**, *27*, e400–e404. [[CrossRef](#)] [[PubMed](#)]
35. Fink, D.; Zheng, H.; Nebel, S.; Norris, P.S.; Aebi, S.; Lin, T.P.; Nehmé, A.; Christen, R.D.; Haas, M.; MacLeod, C.L.; et al. In Vitro and in Vivo Resistance to Cisplatin in Cells That Have Lost DNA Mismatch Repair. *Cancer Res.* **1997**, *57*, 1841–1845. [[PubMed](#)]
36. Zhao, P.; Li, L.; Jiang, X.; Li, Q. Mismatch repair deficiency/microsatellite instability-high as a predictor for anti-PD-1/PD-L1 immunotherapy efficacy. *J. Hematol. Oncol.* **2019**, *12*, 54. [[CrossRef](#)] [[PubMed](#)]
37. Liu, J.Y.; Qian, C.Y.; Gao, Y.F.; Chen, J.; Zhou, H.H.; Yin, J.Y. Association between DNA mismatch repair gene polymorphisms and platinum-based chemotherapy toxicity in non-small cell lung cancer patients. *Chin. J. Cancer* **2017**, *36*, 12. [[CrossRef](#)]
38. Landau, D.A.; Slack, F.J. MicroRNAs in mutagenesis, genomic instability, and DNA repair. *Semin. Oncol.* **2011**, *38*, 743–751. [[CrossRef](#)]
39. Song, Y.; Zuo, Y.; Qian, X.L.; Chen, Z.P.; Wang, S.K.; Song, L.; Peng, L.P. Inhibition of MicroRNA-21-5p Promotes the Radiation Sensitivity of Non-Small Cell Lung Cancer Through HMSH2. *Cell. Physiol. Biochem.* **2017**, *43*, 1258–1272. [[CrossRef](#)]
40. Chao, T.F.; Xiong, H.H.; Liu, W.; Chen, Y.; Zhang, J.X. MiR-21 mediates the radiation resistance of glioblastoma cells by regulating PDCD4 and hMSH2. *J. Huazhong Univ. Sci. Technol. Med. Sci.* **2013**, *33*, 525–529. [[CrossRef](#)] [[PubMed](#)]
41. Valeri, N.; Gasparini, P.; Braconi, C.; Paone, A.; Lovat, F.; Fabbri, M.; Sumani, K.M.; Alder, H.; Amadori, D.; Patel, T.; et al. MicroRNA-21 induces resistance to 5-fluorouracil by down-regulating human DNA MutS homolog 2 (hMSH2). *Proc. Natl. Acad. Sci. USA* **2010**, *107*, 21098–21103. [[CrossRef](#)] [[PubMed](#)]
42. Zhong, Z.; Dong, Z.; Yang, L.; Gong, Z. miR-21 induces cell cycle at S phase and modulates cell proliferation by down-regulating hMSH2 in lung cancer. *J. Cancer Res. Clin. Oncol.* **2012**, *138*, 1781–1788. [[CrossRef](#)] [[PubMed](#)]
43. Yamamoto, H.; Adachi, Y.; Taniguchi, H.; Kunimoto, H.; Noshio, K.; Suzuki, H.; Shinomura, Y. Interrelationship between microsatellite instability and microRNA in gastrointestinal cancer. *World J. Gastroenterol.* **2012**, *18*, 2745–2755. [[CrossRef](#)]
44. Mao, G.; Lee, S.; Ortega, J.; Gu, L.; Li, G.M. Modulation of microRNA processing by mismatch repair protein MutL α . *Cell Res.* **2012**, *22*, 973–985. [[CrossRef](#)] [[PubMed](#)]

45. Yu, Y.; Wang, Y.; Ren, X.; Tsuyada, A.; Li, A.; Liu, L.J.; Wang, S.E. Context-dependent bidirectional regulation of the MutS homolog 2 by transforming growth factor β contributes to chemoresistance in breast cancer cells. *Mol. Cancer Res.* **2010**, *8*, 1633–1642. [[CrossRef](#)] [[PubMed](#)]
46. Valeri, N.; Gasparini, P.; Fabbri, M.; Braconi, C.; Veronese, A.; Lovat, F.; Adair, B.; Vannini, I.; Fanini, F.; Bottoni, A.; et al. Modulation of mismatch repair and genomic stability by miR-155. *Proc. Natl. Acad. Sci. USA* **2010**, *107*, 6982–6987. [[CrossRef](#)] [[PubMed](#)]
47. Manikandan, M.; Deva Magendhra Rao, A.K.; Rajkumar, K.S.; Rajaraman, R.; Munirajan, A.K. Altered levels of miR-21, miR-125b-2*, miR-138, miR-155, miR-184, and miR-205 in oral squamous cell carcinoma and association with clinicopathological characteristics. *J. Oral Pathol. Med.* **2015**, *44*, 792–800. [[CrossRef](#)] [[PubMed](#)]
48. Lubov, J.; Maschietto, M.; Ibrahim, I.; Mlynarek, A.; Hier, M.; Kowalski, L.P.; Alaoui-Jamali, M.A.; da Silva, S.D. Meta-analysis of microRNAs expression in head and neck cancer: Uncovering association with outcome and mechanisms. *Oncotarget* **2017**, *8*, 55511–55524. [[CrossRef](#)]
49. Kumarasamy, C.; Madhav, M.R.; Sabarimurugan, S.; Krishnan, S.; Baxi, S.; Gupta, A.; Gothandam, K.M.; Jayaraj, R. Prognostic Value of miRNAs in Head and Neck Cancers: A Comprehensive Systematic and Meta-Analysis. *Cells* **2019**, *8*, 772. [[CrossRef](#)]
50. Li, W.-Q.; Zhang, J.-P.; Wang, Y.-Y.; Li, X.-Z.; Sun, L. MicroRNA-422a functions as a tumor suppressor in non-small cell lung cancer through SULF2-mediated TGF- β /SMAD signaling pathway. *Cell Cycle* **2019**, *18*, 1727–1744. [[CrossRef](#)]
51. Shao, C.; Yang, F.; Qin, Z.; Jing, X.; Shu, Y.; Shen, H. The value of miR-155 as a biomarker for the diagnosis and prognosis of lung cancer: A systematic review with meta-analysis. *BMC Cancer* **2019**, *19*, 1103. [[CrossRef](#)]
52. Hetta, H.F.; Zahran, A.M.; Shafik, E.A.; El-Mahdy, R.I.; Mohamed, N.A.; Nabil, E.E.; Esmael, H.M.; Alkady, O.A.; Elkady, A.; Mohareb, D.A.; et al. Circulating miRNA-21 and miRNA-23a Expression Signature as Potential Biomarkers for Early Detection of Non-Small-Cell Lung Cancer. *MicroRNA* **2019**, *8*, 206–215. [[CrossRef](#)]
53. Li, S.; Zeng, X.; Ma, R.; Wang, L. MicroRNA-21 promotes the proliferation, migration and invasion of non-small cell lung cancer A549 cells by regulating autophagy activity via AMPK/ULK1 signaling pathway. *Exper. Med.* **2018**, *16*, 2038–2045. [[CrossRef](#)]
54. Xu, S.; Shi, L. High expression of miR-155 and miR-21 in the recurrence or metastasis of non-small cell lung cancer. *Oncol. Lett.* **2019**, *18*, 758–763. [[CrossRef](#)] [[PubMed](#)]
55. Silantyyev, A.S.; Falzone, L.; Libra, M.; Gurina, O.I.; Kardashova, K.S.; Nikolouzakis, T.K.; Nosyrev, A.E.; Sutton, C.W.; Mitsias, P.D.; Tsatsakis, A. Current and Future Trends on Diagnosis and Prognosis of Glioblastoma: From Molecular Biology to Proteomics. *Cells* **2019**, *8*, 863. [[CrossRef](#)] [[PubMed](#)]
56. Tuaeava, N.O.; Falzone, L.; Porozov, Y.B.; Nosyrev, A.E.; Trukhan, V.M.; Kovatsi, L.; Spandidos, D.A.; Drakoulis, N.; Kalogeraki, A.; Mamoulakis, C.; et al. Translational Application of Circulating DNA in Oncology: Review of the Last Decades Achievements. *Cells* **2019**, *8*, 1251. [[CrossRef](#)] [[PubMed](#)]
57. Sasaki, C.T.; Doukas, S.G.; Vageli, D.P. In Vivo Short-Term Topical Application of BAY 11-7082 Prevents the Acidic Bile-Induced mRNA and miRNA Oncogenic Phenotypes in Exposed Murine Hypopharyngeal Mucosa. *Neoplasia (New York, N.Y.)* **2018**, *20*, 374–386. [[CrossRef](#)] [[PubMed](#)]
58. Doukas, S.G.; Cardoso, B.; Tower, J.I.; Vageli, D.P.; Sasaki, C.T. Biliary tumorigenic effect on hypopharyngeal cells is significantly enhanced by pH reduction. *Cancer Med.* **2019**, *8*, 4417–4427. [[CrossRef](#)]
59. Vageli, D.P.; Doukas, S.G.; Spock, T.; Sasaki, C.T. Curcumin prevents the bile reflux-induced NF- κ B-related mRNA oncogenic phenotype, in human hypopharyngeal cells. *J. Cell. Mol. Med.* **2018**, *22*, 4209–4220. [[CrossRef](#)] [[PubMed](#)]
60. Doukas, P.G.; Vageli, D.P.; Doukas, S.G.; Sasaki, C.T. Temporal characteristics of NF- κ B inhibition in blocking bile-induced oncogenic molecular events in hypopharyngeal cells. *Oncotarget* **2019**, *10*, 3339–3351. [[CrossRef](#)]
61. Hecht, S.S.; Rivenson, A.; Braley, J.; DiBello, J.; Adams, J.D.; Hoffmann, D. Induction of oral cavity tumors in F344 rats by tobacco-specific nitrosamines and snuff. *Cancer Res.* **1986**, *46*, 4162–4166.
62. Ge, G.Z.; Xu, T.R.; Chen, C. Tobacco carcinogen NNK-induced lung cancer animal models and associated carcinogenic mechanisms. *Acta Biochim. Biophys. Sin. (Shanghai)* **2015**, *47*, 477–487. [[CrossRef](#)]
63. Parsons, A.; Daley, A.; Begh, R.; Aveyard, P. Influence of smoking cessation after diagnosis of early stage lung cancer on prognosis: Systematic review of observational studies with meta-analysis. *BMJ* **2010**, *340*, b5569. [[CrossRef](#)]

64. Day, G.L.; Blot, W.J.; Shore, R.E.; McLaughlin, J.K.; Austin, D.F.; Greenberg, R.S.; Liff, J.M.; Preston-Martin, S.; Sarkar, S.; Schoenberg, J.B.; et al. Second cancers following oral and pharyngeal cancers: Role of tobacco and alcohol. *J. Natl. Cancer Inst.* **1994**, *86*, 131–137. [[CrossRef](#)] [[PubMed](#)]
65. Tom, W.; Nederlof, P.M.; van den Brekel, M.W.; van't Veer, L.J.; de Jong, D.; Hart, A.A.; van Zandwijk, N.; Klomp, H.; Balm, A.J.; van Velthuysen, M.L. Pulmonary Squamous Cell Carcinoma following Head and Neck Squamous Cell Carcinoma: Metastasis or Second Primary? *Clin. Cancer Res.* **2005**, *11*, 6608–6614.
66. Yan, W.; Wistuba, I.I.; Emmert-Buck, M.R.; Erickson, H.S. Squamous Cell Carcinoma - Similarities and Differences among Anatomical Sites. *Am. J. Cancer Res.* **2011**, *1*, 275–300. [[PubMed](#)]
67. Schembri, F.; Sridhar, S.; Perdomo, C.; Gustafson, A.M.; Zhang, X.; Ergun, A.; Lu, J.; Liu, G.; Zhang, X.; Bowers, J.; et al. MicroRNAs as modulators of smoking-induced gene expression changes in human airway epithelium. *Proc. Natl. Acad. Sci. USA* **2009**, *106*, 2319–2324. [[CrossRef](#)] [[PubMed](#)]
68. Mathis, C.; Poussin, C.; Weisensee, D.; Gebe, S.; Hengstermann, A.; Sewer, A.; Belcastro, V.; Xiang, Y.; Ansari, S.; Wagner, S.; et al. Human bronchial epithelial cells exposed in vitro to cigarette smoke at the air-liquid interface resemble bronchial epithelium from human smokers. *Am. J. Physiol. Lung Cell. Mol. Physiol.* **2013**, *304*, 489–503. [[CrossRef](#)]
69. Krishnan, A.R.; Zheng, H.; Kwok, J.G.; Qu, Y.; Zou, A.E.; Korrapati, A.; Li, P.X.; Califano, J.A.; Hovell, M.F.; Wang-Rodriguez, J.; et al. A comprehensive study of smoking-specific microRNA alterations in head and neck squamous cell carcinoma. *Oral Oncol.* **2017**, *72*, 56–64. [[CrossRef](#)]
70. Irimie-Aghiorghiesei, A.I.; Pop-Bica, C.; Pinteau, S.; Braicu, C.; Cojocneanu, R.; Zimța, A.A.; Gulei, D.; Slabý, O.; Berindan-Neagoe, I. Prognostic Value of MiR-21: An Updated Meta-Analysis in Head and Neck Squamous Cell Carcinoma (HNSCC). *J. Clin. Med.* **2019**, *8*, 2041. [[CrossRef](#)]
71. Zheng, W.; Zhao, J.; Tao, Y.; Guo, M.; Ya, Z.; Chen, C.; Qin, N.; Zheng, J.; Luo, J.; Xu, L. MicroRNA-21: A promising biomarker for the prognosis and diagnosis of non-small cell lung cancer. *Oncol. Lett.* **2018**, *16*, 2777–2782. [[CrossRef](#)]
72. Cheng, A.M.; Byrom, M.W.; Shelton, J.; Ford, L.P. Antisense inhibition of human miRNAs and indications for an involvement of miRNA in cell growth and apoptosis. *Nucleic Acids Res.* **2005**, *33*, 1290–1297. [[CrossRef](#)]
73. International Agency for Research on Cancer Smokeless tobacco and some tobacco-specific N-nitrosamines. *IARC Monogr. Eval. Carcinog. Risks Hum.* **2007**, *89*, 419–548.
74. Hecht, S.S. Tobacco carcinogens, their biomarkers and tobacco-induced cancer. *Nat. Rev. Cancer* **2003**, *3*, 733–744. [[CrossRef](#)] [[PubMed](#)]
75. Downey, C.M.; Jirik, F.R. DNA mismatch repair deficiency accelerates lung neoplasm development in K-rasLA1/+ mice: A brief report. *Cancer Med.* **2015**, *4*, 897–902. [[CrossRef](#)] [[PubMed](#)]
76. Brown, P.J.; Bedard, L.L.; Massey, T.E. Repair of 4-(methylnitrosamino)-1-(3-pyridyl)-1-butanone-induced DNA pyridyloxobutylation by nucleotide excision repair. *Cancer Lett.* **2008**, *260*, 48–55. [[CrossRef](#)] [[PubMed](#)]
77. Brown, P.J.; Massey, T.E. In vivo treatment with 4-(methylnitrosamino)-1-(3-pyridyl)-1-butanone (NNK) induces organ-specific alterations in in vitro repair of DNA pyridyloxobutylation. *Mutat. Res.* **2009**, *663*, 15–21. [[CrossRef](#)]
78. Westwood, A.; Glover, A.; Hutchins, G.; Young, C.; Brockmoeller, S.; Robinson, R.; Worrielow, L.; Wallace, D.; Rankeillor, K.; Adlard, J.; et al. Additional loss of MSH2 and MSH6 expression in sporadic deficient mismatch repair colorectal cancer due to MLH1 promoter hypermethylation. *J. Clin. Pathol.* **2019**, *72*, 443–447. [[CrossRef](#)]
79. Kang, Z.; Zhu, Y.; Zhang, Q.A.; Dong, L.; Xu, F.; Zhang, X.; Guan, M. Methylation and expression analysis of mismatch repair genes in extramammary Paget's disease. *J. Eur. Acad. Derm. Venereol.* **2019**, *33*, 874–879. [[CrossRef](#)]
80. Bhattacharjee, P.; Sanyal, T.; Bhattacharjee, S.; Bhattacharjee, P. Epigenetic alteration of mismatch repair genes in the population chronically exposed to arsenic in West Bengal, India. *Env. Res.* **2018**, *163*, 289–296. [[CrossRef](#)]
81. Wang, S.; Wu, W.; Claret, F.X. Mutual regulation of microRNAs and DNA methylation in human cancers. *Epigenetics* **2017**, *12*, 187–197. [[CrossRef](#)]
82. Sandoval, J.; Díaz-Lagares, A.; Salgado, R.; Servitje, O.; Climent, F.; Ortiz-Romero, P.L.; Pérez-Ferriols, A.; Garcia-Muret, M.P.; Estrach, T.; Garcia, M.; et al. MicroRNA Expression Profiling and DNA Methylation Signature for Deregulated MicroRNA in Cutaneous T-Cell Lymphoma. *J. Investig. Derm.* **2015**, *135*, 1128–1137. [[CrossRef](#)]

83. Ortiz, I.M.D.P.; Barros-Filho, M.C.; Dos Reis, M.B.; Beltrami, C.M.; Marchi, F.A.; Kuasne, H.; Do Canto, L.M.; De Mello, J.B.H.; Abildgaard, C.; Pinto, C.A.L.; et al. Loss of DNA methylation is related to increased expression of miR-21 and miR-146b in papillary thyroid carcinoma. *Clin. Epigenet.* **2018**, *10*, 144. [CrossRef]
84. Krzeminski, P.; Sarasquete, M.E.; Misiewicz-Krzeminska, I.; Corral, R.; Corchete, L.A.; Martín, A.A.; García-Sanz, R.; San Miguel, J.F.; Gutiérrez, N.C. Insights into epigenetic regulation of microRNA-155 expression in multiple myeloma. *Biochim. Biophys. Acta* **2015**, *1849*, 353–366. [CrossRef]
85. Chen, Y.J.; Luo, J.; Yang, G.Y.; Yang, K.; Wen, S.Q.; Zou, S.Q. Mutual regulation between microRNA-373 and methyl-CpG-binding domain protein 2 in hilar cholangiocarcinoma. *World J. Gastroenterol.* **2012**, *18*, 3849–3861. [CrossRef]
86. Gate, L.; Tew, K.D. Alkylating Agents. In *Cancer Management in Man: Chemotherapy, Biological Therapy, Hyperthermia and Supporting Measures*; Cancer Growth and Progression; Mineev, B.R., Ed.; Springer: Dordrecht, The Netherlands; Moores UCSD Cancer Center: La Jolla, CA, USA, 2011; Volume 13, pp. 61–85.
87. Tsatsakis, A.; Docea, A.O.; Constantin, C.; Calina, D.; Zlatian, O.; Nikolouzakis, T.K.; Stivaktakis, P.D.; Kalogeraki, A.; Liesivuori, J.; Tzanakakis, G.; et al. Genotoxic, cytotoxic, and cytopathological effects in rats exposed for 18 months to a mixture of 13 chemicals in doses below NOAEL levels. *Toxicol. Lett.* **2019**, *316*, 154–170. [CrossRef]
88. Tsatsakis, A.M.; Kouretas, D.; Tzatzarakis, M.N.; Stivaktakis, P.; Tsarouhas, K.; Golokhvast, K.S.; Rakitskii, V.N.; Tutelyan, V.A.; Hernandez, A.F.; Rezaee, R.; et al. Simulating real-life exposures to uncover possible risks to human health: A proposed consensus for a novel methodological approach. *Hum. Exp. Toxicol.* **2017**, *36*, 554–564. [CrossRef]
89. Pierceall, W.E.; Olaussen, K.A.; Rousseau, V.; Brambilla, E.; Sprott, K.M.; Andre, F.; Pignon, J.P.; Le Chevalier, T.; Pirker, R.; Jiang, C.; et al. Cisplatin benefit is predicted by immunohistochemical analysis of DNA repair proteins in squamous cell carcinoma but not adenocarcinoma: Theranostic modeling by NSCLC constituent histological subclasses. *Ann. Oncol.* **2012**, *23*, 2245–2252. [CrossRef]
90. Kamal, N.S.; Soria, J.C.; Mendiboure, J.; Planchard, D.; Olaussen, K.A.; Rousseau, V.; Popper, H.; Pirker, R.; Bertrand, P.; Dunant, A.; et al. International Adjuvant Lung Trial-Bio investigators. MutS homologue 2 and the long-term benefit of adjuvant chemotherapy in lung cancer. *Clin. Cancer Res.* **2010**, *16*, 1206–1215.
91. Hause, R.J.; Pritchard, C.C.; Shendure, J.; Salipante, S.J. Classification and characterization of microsatellite instability across 18 cancer types. *Nat. Med.* **2016**, *22*, 1342–1350. [CrossRef]
92. Chang, L.; Chang, M.; Chang, H.M.; Chang, F. Microsatellite Instability: A Predictive Biomarker for Cancer Immunotherapy. *Appl. Immunohistochem. Mol. Morphol.* **2018**, *26*, e15–e21. [CrossRef] [PubMed]

